Title page

Dual Targeting of DNA and EGFR by ZYH005: A Novel Strategy to Induce DNA Damage and Inhibit EGFR-WEE1 Interaction in Glioblastoma Treatment

Jianzheng Huang[1], Zijun Zhang[1], Yang Xiao[1], Ziming Zhao[1], Zengwei Luo[1], Chao Song[2], Shouchang Feng[3], Suojun Zhang[3], Xingjiang Yu[2], Qingyi Tong[1,*], Yonghui Zhang[1,*]

[1]Department of Hubei Key Laboratory of Natural Medicinal Chemistry and Resource Evaluation, School of Pharmacy, Tongji Medical College, Huazhong University of Science and Technology, Wuhan, 430030, China;

[2]Department of Histology and Embryology, School of Basic Medicine, Tongji Medical College, Huazhong University of Science and Technology, Wuhan, China;

[3]Department of Neurosurgery, Tongji Hospital, Tongji Medical College, Huazhong University of Science and Technology, Wuhan, China.

Corresponding Author: Yonghui Zhang, Department of Hubei Key Laboratory of Natural Medicinal Chemistry and Resource Evaluation, School of Pharmacy, Tongji Medical College, Huazhong University of Science and Technology, 13 Hangkong Road, Jianghan District, Wuhan, Hubei Province, 430030, China (zhangyh@mails.tjmu.edu.cn.); Qingyi

Tong, Department of Hubei Key Laboratory of Natural Medicinal Chemistry and Resource Evaluation, School of Pharmacy, Tongji Medical College, Huazhong University of Science and Technology, 13 Hangkong Road, Jianghan District, Wuhan, Hubei Province, 430030, China (qytong@hust.edu.cn.);

Abstract

Background: Glioblastoma (GBM) is a highly aggressive malignancy with limited therapeutic option. EGFR and WEE1 play specific roles in the occurrence and development of GBM and are potential therapeutic targets for it. ZYH005 (Z5) is a DNA intercalator with low systemic toxicity and enhanced blood-brain barrier penetration, its therapeutic efficacy and underlying mechanisms in GBM are worth further exploration.

Methods: The antitumor efficacy of Z5 was determined with GBM cell lines and patient-derived glioblastoma stem cells (GSCs) in vitro and in vivo through cell proliferation, colony formation and western blots assays. The targets of Z5 and related mechanisms were validated using CMap, DNA microarrays and surface plasmon resonance (SPR).

Results: Z5 demonstrated robust anti-proliferative activity against both conventional GBM cell lines and patient-derived glioblastoma stem cells (GSCs), while significantly suppressing orthotopic tumor growth and

prolonging survival in murine models. Mechanistic studies revealed a dual mechanism of action: Z5 directly induces persistent DNA damage and inhibits DNA repair pathways, while simultaneously binding to EGFR's Glu762 residue to disrupt its interaction with WEE1. This interference blocks WEE1 phosphorylation at Ser642, abrogating G2/M checkpoint activation and triggering mitotic catastrophe in cells.

Conclusions: These results clearly demonstrate the dual functionality of Z5, which serves as both a DNA intercalator and an EGFR inhibitor. In GBM cells, Z5 effectively induces mitotic catastrophe, and in GSCs-based models, it exhibits remarkable anti - tumor activity. Consequently, Z5 stands out as a highly promising candidate for the development of innovative GBM treatments.

Keywords: Glioblastoma; EGFR-WEE1 axis; mitotic catastrophe; DNA intercalator

Introduction

Glioblastoma multiforme (GBM) stands as the most invasive and deadly primary brain tumor among adults[1]. It constitutes around 49% of all malignant central nervous system tumors. In high-income countries, its annual incidence is 3-7 cases per 100,000 individuals[2,3]. The treatment of GBM adopts a multimodal strategy, integrating surgery, radiotherapy, and temozolomide (TMZ)-based chemotherapy. However, the median survival time for GBM patients is a mere 12-16 months, and the 5-year

survival rate remains below 5%[2,3]. This persistent therapeutic impasse underscores the critical need for paradigm-shifting treatment strategies in neuro-oncology.

The development of DNA-targeted anti-cancer drugs represents a classic treatment strategy. It makes full use of the differences in DNA damage response (DDR) between normal cells and cancer cells, including differences in the integrity of the DDR pathway, variations in replication rates, and changes in the level of accumulated DNA damage, among others[4-6]. Numerous studies have shown that due to the dysregulation of the DDR pathway, GBM is inherently resistant to radiotherapy and chemotherapy. Targeted inhibition of the activation of the DDR pathway and the exacerbation of replication stress are effective strategies for improving the prognosis of GBM patients and overcoming treatment resistance[7]. In addition, as the cornerstone of chemotherapy for GBM, TMZ is also a DNA-targeted drug. Its mechanism of action is to alkylate DNA by binding to it and cause DNA damage[6,8]. On this basis, combining other DNA-damaging drugs and DDR inhibitors with standard therapies such as TMZ or immunotherapies is expected to increase the unique genomic instability of GBM and enhance the effectiveness of combination therapies.

There are many proteins related to DDR, but in GBM, EGFR and WEE1 are two that deserve special attention. EGFR is frequently

amplified or mutated in GBM, driving uncontrolled proliferation and survival[9]. EGFR signaling can activate DDR pathways, enabling tumor cells to repair therapy-induced DNA damage. Conversely, DNA damage may upregulate EGFR expression, allowing the cell to survive[10-12]. WEE1, a canonical G2/M checkpoint protein, is pivotal in this cellular process. When DNA damage occurs, ATM and ATR kinases indirectly activate WEE1. Activated WEE1 phosphorylates CDK1, arresting the cell cycle at the G2/M transition. This arrest gives the cell time to repair DNA damage before mitosis, highlighting WEE1's role in maintaining genomic integrity[13]. Preclinical studies show that WEE1 inhibitors like MK-1775 potentiate the effects of radiation and various DNA-damaging agents, including temozolomide in GBM models[13,14]. Consequently, the intricate relationships among DNA damage, EGFR, and WEE1 are of paramount importance and must not be underestimated. Beyond the conventional strategies centered around targeting DNA and the DDR, the therapeutic approach of treating GBM by inhibiting the EGFR and WEE1 is a highly promising drug-development avenue worthy of in-depth exploration.

Phenanthridinone is an important class of heterocyclic structures, which widely exist in the bioactive alkaloids[15]. It also serves as a parent nucleus structure holding immense potential in the realm of anti-tumor drug development[16,17]. Nevertheless, these natural products are scarce and hard to obtain. We've developed a novel, eco-friendly, cost-effective

synthetic method for the phenanthridone scaffold [30]. It enables large-scale synthesis of its derivatives (patent pended) and resolved the supply bottlenecks in this field[18]. Then, we synthesized several new phenanthridone derivatives and found that the crinasiadine-type derivative ZYH005 (Z5) had the strongest anticancer activity[17]. Notably, natural crinasiadine has weak antitumor activity[15], but Z5 exhibits widely antitumor activity, even stronger than the well-known phenanthridone alkaloid narciclasine. As reported, narciclasine can only induce leukemia cells apoptosis at concentrations greater than 1 μM after 48 hours of treatment [19-21], whereas Z5 can induce apoptosis after 6 hours of treatment at 50 nM[17]. In tumor-bearing mouse models, at safe doses, narciclasine significantly inhibited the growth of primary GBM, brain-metastatic melanoma, and lung cancer, but not that of other cancer types[19,20]. Given its relatively strong lipophilicity, which enables it to cross the blood-brain barrier (BBB), narciclasine is regarded as a potential candidate drug for GBM[21]. Structurally, Z5 has fewer hydrophilic (hydroxyl) groups, so its lipophilicity is theoretically higher than that of narciclasine. Accordingly, we assessed the BBB permeability in mice and found Z5 outperforms narciclasine (Supplementary Figures S1A-D). However, the anti-GBM effects and underlying mechanisms of this novel, more potent phenanthridone derivatives remain uninvestigated.

In the present study, we clearly demonstrated that Z5 exerts a

significant inhibitory effect on GBM cells and glioblastoma stem cells (GSCs) in vitro and in vivo. Notably, we identify Z5 as a direct binder of EGFR's Glu762 and reveal its disruption of the EGFR-WEE1 interaction via Glu762 and Ser642 in GBM cells, inhibiting downstream signaling. By inducing DNA damage and targeting the EGFR-WEE1 axis, Z5 demonstrates substantial efficacy in GBM. This study lays the foundation for the further development of Z5 as a lead compound and represents a new exploration in the development of effective therapeutic drugs for GBM.

Materials and Methods

DNA fragment detection assay

Cells were seeded into 6-well plates and incubated either with or without Z5. After 24 hours, the cells were washed once with cold PBS. Genomic DNA was extracted using the Universal Genomic DNA Purification Mini Spin Kit, as per the manufacturer's instructions. DNA fragment detection was performed as previously published [22]. Briefly, a mixture of DNA, TdT, and dATP was prepared and incubated at 37℃ for 30 minutes, followed by an additional incubation at 75℃ for 20 minutes. Finally, Endo IV and the probe were added to the system. The fluorescence intensity was measured immediately using the real-time PCR instrument (RRID: SCR_018018).

DNA Microarrays and Gene Set Enrichment Analysis (GSEA) analysis

Total RNA samples were extracted from U87-MG cells using the Trizol reagent (Cat#15596-018, Life Technologies, Carlsbad, CA, US) reagent. RNA purification was performed using the NucleoSpin RNA Clean-up XS kit (Cat#740903, MN, Germany) and the RNase-Free DNase Set (Cat#79254, QIAGEN, GmBH, Germany). According to the Affymetrix technical manual, the double-stranded cDNA was hybridized with biotin-labeled fragmented cRNA. Microarray experiments were performed using Affymetrix chips by Shanghai Biotechnology Corporation. Raw data were normalized using the Expression Console algorithm in Command Console Software 4.0 (Affymetrix, Santa Clara, CA, US). Differential expression analysis was conducted using the affy package in R. Genes with an absolute log2 fold change >1 and a P-value <0.05 were considered differentially expressed. The microarray data for U87-MG cells has been submitted to the NGDC/OMIX under accession number OMIX008765. Significantly differentially expressed genes ($|Log2FC| \geq 1$, $FDR \leq 0.05$) are listed in **Supplementary Table S1**. All genes identified through DNA microarray analysis were imported into GSEA software for further analysis and visualization.

Connectivity map (CMAP) analysis

Input the top 66 upregulated genes and 150 downregulated genes in supplementary S1 into the CMAP website (https://clue.io), query parameters were gene expression (L1000), touchstone, individual query, 1.0. The detailed list was sorted by cell types and perturbagen type was compound. The results obtained from CMAP are presented in **Supplementary Tables S2-S11**.

Cellular Thermal Shift Assay (CETSA)

After freeze-thawing the GBM cells twice using liquid nitrogen to get the whole protein, divide the protein solution into two equal parts. Incubate each part with DMSO or Z5 at room temperature for 1 hour. After incubation, aliquot the protein solution and incubate at different temperatures for three minutes. Following this, centrifuge the samples at 12000g, collect the supernatants, and perform immunoblotting analysis.

Drug Affinity Responsive Target Stability Assay (DARTS)

DARTS was performed as previously published[23]. Briefly, after lysing GBM cells with RIPA buffer, divide the protein solution into five equal parts, with each portion being 90 μL. Measure the protein concentration using the BCA kit. Meanwhile, incubate each portion of the protein solution with DMSO or different concentrations of Z5 at room

temperature for 15 minutes. Based on the protein concentration, add protease solution at a ratio of 1:700 (enzyme: protein) and incubate at room temperature for 10 minutes. Subsequently, stop the reaction by adding a protease inhibitor cocktail and SDS-PAGE loading buffer followed by immunoblotting.

Surface plasmon resonance (SPR)

A Biacore 1K instrument was used to measure the binding kinetics of the human EGFR kinase domain (EGFR residues 704-1016) and human WEE1 kinase domain (WEE1 residues 293-568) to Z5. Measurements were performed at 25□. Proteins were dissolved in PBS, pH7.4. The proteins were immobilized on the CM5 sensor chip (Cytiva, 29149603, Shanghai, China) using the amine-coupling method according to standard protocols. Data were processed using standard double-referencing and fit to a 1:1 binding model using Biacore 1K Evaluation software. The association rate (K_{on}, M^{-1}□s^{-1}), dissociation rate (K_{off}, s^{-1}), estimate of error (SE), Chi-Square (Chi^2), and statistic and maximum response (R_{max}) and response units (RU) were determined. The equilibrium dissociation constant (K_d) was calculated from the relationship K_D□=□K_{off}/K_{on} (M).

Lip-MS

Lip-MS was performed as previously published[24]. A detailed description

is in **Supplementary Material**.

Molecular Docking

Molecular docking studies were performed using Schrödinger Maestro (Schrödinger Release 2023-1: Maestro, Schrödinger, LLC, New York, NY, 2023). Protein models were retrieved from the Protein Data Bank (PDB) and optimized through the Protein Preparation Workflow module. The structure of Z5 was preprocessed with the LigPrep module. The docking grid focused on the substrate-binding site of the target protein, utilizing standard precision settings for ligand docking under default parameters. Post-docking interaction analyses and alignments were visualized and conducted using PyMOL software.

EGFR and WEE1 complexes prediction

For EGFR and WEE1 complexes prediction, we utilized the AF3 server (https://alphafoldserver.com/). The sequences of EGFR (P00533-1) and WEE1 (P30291-1) were obtained from the Uniprot database. The subsequent docking analysis was performed using PyMOL software.

Orthotopic Transplantation mouse model assay

Experimental Balb/c nude mice were purchased from Beijing Vital River Laboratory Animal Technology Co., Ltd (Beijing, China) and kept at the

Experimental Animal Center of Tongji Medical College, Huazhong University of Science and Technology, Wuhan, China. All mice underwent phenobarbital sodium anesthesia before surgery. One week after GSC ($2x10^4$ cells/mouse) was implanted in the right frontal lobe of 4-week-old mice, 15 mice were randomly divided into three groups: NT, Z5-L (10mg/kg) and Z5-H (20mg/kg). The mice received either solvent (5% DMSO, 20% castor oil, and 75% saline) or varying doses of the drug via gavage for 7 weeks. When the NT group showed the first manifestation of obvious neurological signs, one mouse from each of the remaining two groups was evaluated for drug efficacy. The remaining 12 mice were used for survival studies.

Statistical analysis

Statistical analysis was performed using GraphPad Prism 9.0 software. The data were expressed as the mean ± SD. We used paired t test for statistical analysis between 2 groups, and one-way ANOVA for multiple comparisons. All experiments were repeated more than 3 times. We considered a p-value less than 0.05 to be statistically significant.

Results

3.1 Z5 inhibits the proliferation and induces DNA damage in GBM cells

Viability assessments revealed that Z5 exhibited substantial inhibitory effects on GBM cell proliferation in both time- and dose-dependent manners. Specifically, the 72-hour IC_{50} values were determined to be 0.114 ± 0.016 μM for U87-MG cells and 0.147 ± 0.049 μM for U251-MG cells (Figure 1A). Moreover, Z5 demonstrated a marked ability to reduce colony formation in both cell lines (Figure 1B). Further investigation using EdU staining confirmed that Z5 effectively suppressed cell growth (Figures 1C-D). Given Z5's known mechanism as a DNA intercalator[17], we examined its impact on DNA integrity. Our data show that Z5 significantly increased the number of DNA fragments (Figure 1E) and elevated γ-H2AX expression levels, a marker of DNA damage (Figure 1F). Collectively, these findings strongly indicate that Z5 demonstrates a highly promising capacity for inhibiting proliferation and inducing DNA damage in GBM cells.

3.2 Z5 induces G2/M arrest and mitotic catastrophe in GBM cells

To investigate Z5's mechanism, we designed a microarray-based study. The quantitative analysis revealed that Z5 treatment resulted in 1970 differentially expressed genes (188 upregulated and 1782 downregulated) in U87-MG cells (Supplementary Figure S2A). Among these, the most significantly downregulated genes were *KPNA2*, *PRKDC*, and *MKI67* in U87-MG, with qRT-PCR confirming expression changes for these genes

(Supplementary Figures S2B-C).

Subsequently, we performed KEGG, GO, and GSEA enrichment analyses on the microarray data. Through KEGG and GSEA analyses, we found that Z5 significantly influenced DNA replication pathways. Integrating GOCC and GSEA data further indicated that Z5 primarily functions within the nucleus, replication fork and chromosomal region, suggesting that Z5 still exerts its function as a DNA intercalator in U87-MG cells (Figures 2A-B). As previously observed, Z5 upregulates γ-H2AX expression, so we investigated the impact of DDR on Z5's activity. When DNA is damaged, the cell activates the DDR. This, in turn, triggers DNA repair mechanisms. GSEA analysis, as expected, showed that Z5 significantly inhibited DNA repair pathways (Figure 2C). Next, by adopting the well-known DT40-DDR research model[25], we found that the knockdown of key genes involved in DNA repair (e.g., Rev3 in TLR) increased the efficacy of Z5 (Supplementary Figure S2D). These findings suggest that inhibition of DNA repair pathways may play a facilitative role in enhancing Z5's functional activity.

In addition to its impact on DNA, GSEA analysis revealed that Z5 significantly inhibits the G2M checkpoint, mitotic spindle, and cell cycle pathways (Figure 2C,). Consequently, an investigation into the effects of Z5 on the cell cycle was undertaken. After Z5 treatment for 48 hours, the phosphorylation of WEE1 and its downstream CDC2 is inhibited, and the

expression of PHH3 increases, indicating that the G2/M checkpoint is abolished (Supplementary Figure 2E). Flow cytometry revealed Z5 induced G2/M-phase arrest (4.7-fold PHH3+ cells, $p<0.001$; >4n DNA populations; Figure 2D, Supplementary figures 2F-G). Given that Z5 can both induce DNA damage and trigger G2/M arrest, this led us to consider the possibility of mitotic catastrophe. Immunofluorescence analysis provided conclusive evidence of mitotic catastrophe, characterized by the presence of aberrant chromosomes and multipolar spindles (Figure 2G). Mechanistically, this phenomenon is intricately associated with the dysregulation of the G2/M checkpoint. These results firmly demonstrate that Z5 can induce DNA damage and G2/M arrest in GBM cells, which in turn leads to mitotic catastrophe.

3.3 Z5 targets EGFR

We next analyzed the gene expression data from U87-MG cells using the CMAP database. CMAP is a tool used to discover relationships between drugs, gene expression, and diseases by analyzing gene expression profiles to predict drug effects and potential therapeutic targets[26]. By querying the Connectivity Map with a signature containing the top 66 upregulated genes and the top 150 downregulated genes from microarray data, we obtained positive connectivity scores for compounds. We categorized the obtained data by cell type and selected perturbagen type

as compounds. For each cell type, we identified the top 10 compounds based on their ranking and statistically analyzed their descriptions. The six most frequent descriptions are listed below (Supplementary Tables 2-11, Figure 3A). This suggests that the gene expression changes observed after treatment with Z5 are most similar to EGFR inhibitor in cells. Through GSEA analysis of microarray data, we found that Z5 can inhibit the PI3K/AKT/mTOR pathway and mTORC1 activation (Figure S3A). Additionally, EGFR inhibitors have also been shown to inhibit the PI3K/AKT/mTOR signaling pathway and mTORC1 activation. Given this finding, we hypothesize that Z5 may target EGFR. Using CETSA assays in U87-MG and U251-MG cells, we found that Z5 enhances the thermal stability of EGFR, strongly indicating an interaction between Z5 and EGFR (Figure 3B). Additionally, Z5 increases the enzymatic stability of EGFR in DARTS assay, further supporting this interaction (Figure 3C). Even more compelling evidence comes from SPR experiments, which unequivocally confirmed the direct binding between Z5 and the kinase domain of EGFR. The measured dissociation constant (KD) was determined to be 19.6 μM (Figure 3D). Finally, we examined the effect of Z5 on EGFR and its downstream proteins following treatment. Further confirmed that Z5 significantly reduces the expression levels of p-EGFR, p-ERK, and p-mTOR in U87-MG and U251-MG cells. Conversely, it leads to an upregulation of EGFR expression in U251-MG. (Figure 3E).

To further investigate the specific binding site of Z5 on EGFR, we conducted Lip-MS experiments, given that Z5 binds to EGFR non-covalently. Results of Lip-MS identified potential peptide segments within the EGFR kinase domain where Z5 might bind (Supplementary Figures 3B-C). Subsequently, we performed molecular docking studies by aligning Z5 with various EGFR structures available in the Protein Data Bank. Our analysis revealed that Z5 may bind the GLU-738 residue and MET-769 residues of EGFR (Supplementary Figures 3D-E). By integrating the results of LIP-MS, we have identified GLU-738 as a critical binding site for Z5.

We further validated this outcome with siRNA. First, the interference efficiency of siRNAs targeting EGFR in U87-MG and U251-MG cells were examined. In light of its efficacy, siEGFR-1261 was selected for subsequent experiments (Supplementary Figure S4A). Our results manifested that siRNA-mediated knockdown of EGFR weakened Z5's proliferative inhibition effectiveness in both CCK8 and EdU assays (Figures 3F-G). Moreover, when EGFR was silenced, Z5-induced G2/M arrest vanished, and the upregulation of γ-H2AX and PHH3 proteins was suppressed (Figure 3H-I). Collectively, these findings provide conclusive evidence that EGFR represents a crucial target through which Z5 exerts its anti-GBM effects.

3.4 Z5 interferes with the interaction between EGFR and WEE1

It has been observed that the expression of EGFR is positively correlated with that of WEE1, a key regulator of the G2/M checkpoint, which plays a crucial role in the occurrence of mitotic catastrophe[27,28]. Z5 not only inhibits EGFR function but also downregulates the expression of WEE1 and p-WEE1. We then hypothesize that Z5 might induce mitotic catastrophe by targeting EGFR and subsequently modulating the function of WEE1, leading to the failure of cell cycle regulation.

Our findings revealed that Z5, in tandem with other DNA intercalators like Doxorubicin (DOX) and Daunorubicin (DAU), effectively facilitated the translocation of WEE1 from the nucleus to the cytoplasm (Figure 4A). Subsequently, by immunofluorescence staining, we unexpectedly found that after treatment with Z5, WEE1 diffused out of the nucleus, but EGFR translocated into the nucleus (Figure 4B). Subsequent Co-IP assays confirmed physical EGFR-WEE1 interaction and its attenuation by Z5 (Figure 4C). Subsequently, employing AlphaFold3, we conducted predictions on the interaction between EGFR and WEE1 (Supplementary Figure S5A). Intriguingly, our findings indicate that EGFR's GLU-762 residue interacts with WEE1's SER-642 residue. This GLU-762 site is also proposed as an interaction site for EGFR with Z5. During DNA damage, CHK1 phosphorylates WEE1 at SER-642, which activates the cell cycle checkpoint and prevents cells from entering mitosis. Thus, we

speculate that EGFR may regulate the G2/M cell cycle transition by controlling WEE1 phosphorylation. Moreover, Z5 could interfere with the interaction between EGFR and WEE1, potentially causing mitotic catastrophe in cells. Finally, SPR experiments verified that the kinase domains of EGFR and WEE1 interact with a dissociation constant (KD) value of 17.3 nM (Figure 4D).

Consequently, we aimed to ascertain whether an upstream-downstream relationship exists between EGFR and WEE1. We first disrupted the expression of EGFR and WEE1. The results showed that silencing WEE1 had no impact on the expression of EGFR and p-EGFR. In contrast, silencing EGFR effectively inhibited the expression of WEE1 and p-WEE1 (Figure 4E). Subsequently, by employing MK1775 (a WEE1 inhibitor) and AZD9291 (an EGFR inhibitor), we found that the WEE1 inhibitor had a relatively minor effect on the phosphorylation of EGFR's downstream proteins, ERK and mTOR. However, the EGFR inhibitor could powerfully interfere with the phosphorylation of WEE1 and its downstream protein, CDC2 (Figure 4F). These results lend support to our hypothesis that Z5 reduces the interaction between EGFR and WEE1, inhibiting the phosphorylation of WEE1 and CDC2, leading to the failure of cell cycle regulation.

3.5 Silencing WEE1 significantly impairs the therapeutic efficacy of

Z5

We further verified whether Z5 exerts its anti-GBM effects by targeting the EGFR-WEE1 axis through the silencing of WEE1. Initially, we tested the interference efficiency of siRNAs targeting WEE1 in U87-MG and U251-MG cells and selected siWEE1-1409 for subsequent experiments based on its efficacy (Supplementary Figure S4B). Our results revealed that siRNA-mediated knockdown of WEE1 abrogated Z5's proliferative inhibition efficacy both in CCK8 and EdU assay (Figures 5A-B), and the G2/M cell cycle arrest induced by Z5 (Figure 5C). Additionally, the silencing of WEE1 dampened the Z5-induced upregulation of γ-H2AX and PHH3 protein levels (Figure 5D), providing further confirmation that Z5 exerts its anti-GBM effects by targeting the EGFR-WEE1 axis.

3.6 Z5 suppresses the proliferation of patient-derived GSCs in vitro and in vivo

GSC constitute a distinct subpopulation within glioblastoma, characterized by their stem-like properties and heightened capacity for DNA repair, which confers them with an increased resistance to chemotherapy drugs[29,30]. To investigate the efficacy of Z5 in vivo, we first tested its effects in two cell lines of patient-derived GSCs. Under microscopic examination, it became clear that Z5 exerted a substantial effect in inducing the fragmentation of tumor spheres formed by both

3359 and 456 GSCs lines (Figure 6A-B, Supplementary Figure S6A-B). Subsequently, we carried out immunoblot experiments. The results disclosed that Z5 was capable of markedly suppressing the EGFR-WEE1 axis, in both lines of GSCs. (Figure 6C, Supplementary Figure S6C). Subsequently, we chose the 3359 for further animal studies and established an orthotopic xenograft model in mice. When the first NT (no treatment) mouse neared death, one mouse from each of the three groups was euthanized, and tumor formation was observed through HE staining. The results showed that Z5 significantly inhibited the growth of GSCs within the brain (Figure 6D).

Moreover, Z5 notably prolonged the survival of model mice in a dose-dependent manner. The mean survival time of the mice in the control group was determined to be 102.75 days. For the Z5 - treated groups administered with dosages of 10 mg/kg and 20 mg/kg, the mean survival times of the mice reached 127.5 days and 139 days, representing increases of 24.1% and 35.3% relative to that of the control group, respectively (Figure 6E). IHC staining also demonstrated a significant reduction in EGFR and WEE1 expression within tumors following Z5 treatment (Figure 6F, Supplementary Figures S6D-E). Furthermore, following 8 weeks of Z5 treatment, the results of HE staining showed no signs of toxicity in the heart, liver, spleen, lungs, and kidneys of the mice (Supplementary Figure S7). These findings demonstrate that Z5 not only

effectively inhibits the growth of GSCs in vivo but is also sufficiently safe.

The above results suggest that Z5 is both a DNA intercalator and an EGFR inhibitor. It can induce DNA damage, inhibit EGFR-mediated DNA repair, and suppress the phosphorylation of ERK and mTOR by targeting EGFR. At the same time, it binds to the Glu762 residue of EGFR, disrupts the interaction between EGFR and WEE1, thereby inhibiting the function of WEE1. These combined effects aggravate DNA damage, compelling chromosomes with unrepaired lesions to enter mitosis, resulting in mitotic catastrophe. Under the influence of these comprehensive mechanisms, Z5 demonstrates powerful anti-tumor efficacy in GBM cell lines, GSCs, and orthotopic mouse models of GSCs (Figure 6G).

Discussion

Since TMZ's approval in 2005, despite extensive research over the past decades, no transformative therapies have emerged. Novel therapeutic modalities, including tumor-treating fields, molecularly targeted agents (e.g., EGFR/VEGF inhibitors), and immunotherapy have emerged and begun to be integrated into clinical practice. However, the efficacy of these treatments is significantly limited by tumor heterogeneity, the immunosuppressive tumor microenvironment, and the BBB-mediated

drug exclusion effect, leading to transient remission and high recurrence rates (>90%)[31,32]. Currently, the top-priority task in this field is to spare no effort in the search for new molecules and methods that are effective against GBM. Herein, a novel attempt was made for the early identification of Z5, which possesses potent anti-GBM effects and is sufficiently safe. We also disclosed its mechanism of action, and confirmed that Z5 is a multifunctional compound acting as both DNA intercalator and EGFR inhibitor.

Normal cells have fully functional DDR mechanisms to rapidly detect and repair DNA lesions. In contrast, most cancer cells have defective DDR signaling pathways, and their accelerated proliferation leads to increased DNA damage accumulation. Since the severity of DNA damage is positively correlated with the probability of cell death, malignant cells are more sensitive to DNA-damaging agents. At optimized doses, these drugs can selectively eliminate tumor cells with minimal effects on normal tissues. Several DNA-targeting agents have been approved for clinical use, including platinum-based drugs (cisplatin, carboplatin, oxaliplatin), anthraquinones (mitoxantrone), acridine derivatives (amsacrine), and anthracyclines. Recent breakthroughs in deciphering cancer-specific DNA repair vulnerabilities have reinvigorated this field. Emerging strategies focus on designing next-generation DNA-targeting therapeutics with enhanced potency and tumor specificity, representing a

promising frontier in precision oncology[5,33].

Using single-molecule magnetic tweezers and cell models, we previously confirmed that Z5 is a DNA intercalator[17]. DNA intercalators can reversibly bind to adjacent base pairs of double-stranded DNA (dsDNA), inducing alterations in the structure and multiple functions of the DNA molecule, disrupting its structural stability, and influencing the processing of DNA by other proteins[34,35]. In contrast to alkylating agents, which exert their anticancer effects by irreversibly modifying the DNA structure through covalent bonding, DNA intercalators do not necessarily take immediate effect upon binding to DNA via non-covalent interactions. This is because non-covalent interactions, mainly including van der Waals forces, hydrogen bonds, hydrophobic interactions, and/or charge-transfer forces, render this binding reversible[36]. For these intercalators to exhibit cytotoxic effects, they first need to form a relatively stable complex with a long half-life, which can then interfere with DNA-related enzymes and proteins, thereby affecting processes such as DNA replication, transcription, and translation. Anthracycline drugs, such as doxorubicin and daunorubicin, are typical examples of this mechanism. Although they can intercalate into DNA, their main cytotoxic effect results from the inhibition of topoisomerase II, which prevents the DNA re-ligation step mediated by this enzyme, leading to

DNA strand breaks and cell death. Notably, compared with classic intercalators such as YOYO-1 and ethidium bromide, Z5 is a moderate-strength intercalator. It is implied that the compound may not possess as strong carcinogenic and mutagenic effects as classical intercalators. The in-vitro and in-vivo toxicity assessments of Z5, using different normal cells and mouse models, have confirmed this[17].In this study, the toxicity assessment over an experimental period exceeding 150 days in a GSC-induced orthotopic GBM mouse model also corroborated this finding. In the single-molecule magnetic tweezers experiment, Z5 only causes a moderate degree of change in DNA elongation and twist under low external forces, which partly explains its strong antitumor effect but low toxicity. Meanwhile, this also implies that its mechanism of action may be more complex than simple DNA binding and is worthy of in-depth investigation.

The targets and related mechanisms of Z5 were investigated using classic molecular biology methods. It was confirmed that in addition to being able to induce DNA damage, Z5 is an EGFR inhibitor. Moreover, our hypothesis is that in response to DNA damage, EGFR plays a protective role by modulating the phosphorylation status of WEE1 at the Ser642 residue. This regulation may help maintain cell cycle checkpoints and prevent cells from entering mitosis prematurely. By disrupting the interaction between EGFR and WEE1, Z5 can inhibit EGFR-WEE1 axis

and abrogate G2 phase arrest in cells. Through these mechanisms, Z5 inhibits DNA repair, exacerbates DNA damage, forces chromosomes with unrepaired damage into mitosis, and ultimately induces mitotic catastrophe. These findings are highly consistent with the context of the occurrence and development of GBM. EGFR is frequently amplified (~50% of cases) and mutated in GBM, which drives ligand-independent signaling and tumor progression[37]. EGFR aberrations promote oncogenic phenotypes, including uncontrolled proliferation, angiogenesis, and resistance to apoptosis. Additionally, EGFR alterations contribute to an immunosuppressive tumor microenvironment (TME) by upregulating PD-L1, recruiting immunosuppressive cells, and inhibiting cytotoxic T-cell activity[38]. WEE1 is a cell-cycle checkpoint kinase that phosphorylates CDK1/2 to enforce G2/M arrest, allowing DNA repair before mitosis. In cancer, WEE1 overexpression correlates with poor prognosis and therapeutic resistance, and its inhibition forces mitotic catastrophe in genomic instability cells[39]. GBM cells rely on WEE1 to survive replication stress caused by oncogenic mutations (e.g., EGFR amplification)] and radiation therapy. Preclinical studies have highlighted MK-1775 as radiosensitizers and chemosensitizers in GBM, and combining WEE1 inhibitors with EGFR-targeted therapies may enhance cytotoxicity in EGFRvIII^{+} tumors[27]. Therefore, treating GBM by inhibiting EGFR and WEE1 is a promising direction for drug

development.

Despite preclinical promise, clinical trials targeting EGFR in GBM have largely failed due to redundant signaling pathways and intra tumoral heterogeneity, as well as BBB and immunosuppressive TME[38,40,41]. This severe situation indicates that solely targeting and inhibiting EGFR may not be an effective treatment for GBM. On the other hand, WEE1 inhibition boosts replication stress and genomic instability, selectively targeting p53-deficient GBM cells without harming normal ones. The WEE1 inhibitor MK-1775 enhances TMZ's efficacy, suggesting synergy with DNA-damaging agents and potential for combination therapies[13,27,42].Given the limits of single-agent therapies, combination-therapy approaches are crucial to overcome GBM treatment hurdles. These findings from real-world provide a strong rationale for in-depth research on Z5.

This study has several limitations which we should consider in future research. Previous studies have shown that DNA damage, and DDR activation mediated by EGFR and WEE1 can interact with and crosstalk with each other in cells[9,11,27]. The results of this study cannot precisely distinguish the sequence of events such as Z5-induced DNA damage and the targeted inhibition of EGFR. Therefore, we can only conclude that Z5 negatively regulates the above-mentioned pathways from an overall perspective. Exactly how Z5 precisely affects these pathways still

requires further research relying on more sophisticated cell and molecular biology techniques in the future. Additionally, our research has not yet determined the temporal sequence of Z5 binding to its target proteins and DNA. This requires in-depth research using co-crystallization and mass spectrometry techniques. Last but not least, while EGFR and WEE1 are promising therapeutic targets in various cancers, their relationship has been less explored. In esophageal squamous cell carcinoma (ESCC), although WEE1 expression correlates positively with EGFR levels, the combination of MK1775 with EGFR tyrosine kinase inhibitors has shown limited efficacy across most ESCC cell lines[28]. Given these observations, it is particularly important to understand the complex interactions between EGFR, WEE1, and DNA damage pathways. This prompts us to consider whether the significant efficacy of Z5 stems from its combined actions on DNA damage induction and EGFR-WEE1 inhibition, coupled with its relatively low toxicity profile.

In conclusion, our study for the first time demonstrates the anti-GBM effects and mechanisms of Z5, and reveals that DNA damage, EGFR, and WEE1 can be simultaneously inhibited by a small molecule. This provides a new option for the treatment of GBM, especially in combination therapies. Moreover, for refractory malignancies, rational combinations of DNA intercalators with EGFR and WEE1 inhibitors could represent a viable therapeutic strategy. Z5 also can serve as a lead

compound for investigating the interplay between EGFR, WEE1, and DNA damage.

Conclusions

In this study, we demonstrated that Z5 targets EGFR and disrupts its interaction with WEE1, leading to mitotic catastrophe in glioblastoma multiforme (GBM) cells. Furthermore, our findings suggest that EGFR may regulate the phosphorylation of WEE1 at Ser642, potentially via Glu762. Importantly, treatment with Z5 significantly prolonged the survival of mice bearing orthotopic GSC-derived xenografts. These results highlight the therapeutic potential of Z5 for GBM treatment and provide a novel avenue for future research endeavors.

Declarations

Ethics approval and consent to participate

GSC cells were obtained from glioma patients who underwent surgery at the Department of Neurosurgery of Tongji Hospital, Tongji Medical College of Huazhong University of Science and Technology. All participants provided written informed consent and the study was approved by the Ethics Committee of Tongji Hospital of Tongji Medical College of Huazhong University of Science and Technology (Serial number: 2021-lEC-A244). The Animal Experiment Administration Committee of the Huazhong University of Science and Technology

(HUST) approved all animal experiments to ensure ethical and humane treatment of animals (IACUC Number:3028).

Consent for publication

Not applicable.

Availability of Data and Materials

This study did not generate new regents or original code. All data generated or analyzed during this study are included in this article and its supplementary information files. Microarray data can be accessed through the following link: https://ngdc.cncb.ac.cn/omix/preview/BlYvj2iS.

Competing interests

The authors declare that they have no competing interests.

Funding

This work was financially supported by the by the National Natural Science Foundation of China [grant number 82073886], the Program for Medical Youth Talent of Hubei Province (2024-2027), Hubei Provincial Administration of Traditional Chinese Medicine Research Fund [grant number ZY2023M063], the National Key R&D Program of China [grant number 2021YFA0910500] and National Natural Science Foundation of China [grant number 82473132 and 82072805].

Authors' contributions

Yonghui Zhang and Qingyi Tong conceived the project. Jianzheng Huang performed most of the experiments. Qingyi Tong and Jianzheng Huang prepared the figures, analyzed the data and wrote the manuscript. Zijun Zhang, Yang Xiao, Ziming Zhao and Zengwei Luo participated in some of the experiments. Jianzheng Huang, Chao Song, Xingjiang Yu, Suojun Zhang and Shouchang Feng were responsible for the animal experiments. All authors have read and approved the final manuscript.

Acknowledgements

We thank Dr. Shideng Bao, Dr. Jeremy Rich and Professor Xingjiang Yu for generously providing GSCs (T3359 and D456). We thank the Medical Subcenter of HUST Analytical & Testing Center for acquiring the data, the Experimental Animal Centre of HUST for providing the animal experimentation facilities.

References

1 Weller M, Wen PY, Chang SM, Dirven L, Lim M, Monje M, et al. Glioma. Nature Reviews Disease Primers 2024;10:33.

2 Grochans S, Cybulska AM, Simińska D, Korbecki J, Kojder K,

Chlubek D, et al. Epidemiology of Glioblastoma Multiforme-Literature Review. Cancers 2022;14.

3 Alick P WJJ. A Review of Glioblastoma and Other Primary Brain Malignancies. 2023;330.

4 Cheng B, Pan W, Xing Y, Xiao Y, Chen J, Xu Z. Recent advances in DDR (DNA damage response) inhibitors for cancer therapy. European Journal of Medicinal Chemistry 2022;230:114109.

5 Groelly FJ, Fawkes M, Dagg RA, Blackford AN, Tarsounas M. Targeting DNA damage response pathways in cancer. Nature Reviews Cancer 2023;23:78-94.

6 Roos WP, Thomas AD, Kaina B. DNA damage and the balance between survival and death in cancer biology. Nature Reviews Cancer 2015.

7 Zhen T, Sun T, Xiong B, Liu H, Wang L, Chen Y, et al. New insight into targeting the DNA damage response in the treatment of glioblastoma. Chinese journal of natural medicines 2024;22:869-86.

8 Puigvert J, Sanjiv K, Helleday T. Targeting DNA repair, DNA metabolism and replication stress as anti-cancer strategies. FASEB Journal 2016;283:232-45.

9 Volman Y, Hefetz R, Galun E, Rachmilewitz J. DNA damage alters EGFR signaling and reprograms cellular response via Mre-11. Sci Rep 2022;12:5760.

10 Zubair T, Bandyopadhyay D. Small Molecule EGFR Inhibitors as Anti-Cancer Agents: Discovery, Mechanisms of Action, and Opportunities. 2023;24:2651.

11 Zhou Z, Lu H, Zhu S, Gomaa A, Chen Z, Yan J, et al. Activation of EGFR-DNA-PKcs pathway by IGFBP2 protects esophageal adenocarcinoma cells from acidic bile salts-induced DNA damage. J Exp Clin Cancer Res 2019;38:13.

12 Meyn RE, Munshi A, Haymach JV, Milas L, Ang KK. Receptor signaling as a regulatory mechanism of DNA repair. Radiother Oncol 2009;92:316-22.

13 Bukhari AB, Chan GK, Gamper AM. Targeting the DNA Damage Response for Cancer Therapy by Inhibiting the Kinase Wee1. 2022;12.

14 Hirai H, Arai T, Okada M, Nishibata T, Kobayashi M, Sakai N, et al. MK-1775, a small molecule Wee1 inhibitor, enhances anti-tumor efficacy of various DNA-damaging agents, including 5-fluorouracil. Cancer biology & therapy 2010;9:514-22.

15 Jin Z, Yao G. Amaryllidaceae and Sceletium alkaloids. Natural Product Reports 2019.

16 Azad I, Ahmad R, Khan T, Saquib M, Hassan F, Akhter Y, et al. Phenanthridine derivatives as promising new anticancer agents: synthesis, biological evaluation and binding studies. Future medicinal chemistry 2020;12:709-39.

17 Tong Q, You H, Chen X, Wang K, Sun W, Pei Y, et al. ZYH005, a novel DNA intercalator, overcomes all-trans retinoic acid resistance in acute promyelocytic leukemia. Nucleic Acids Res 2018;46:3284-97.

18 Yuan M, Chen L, Wang J, Chen S, Wang K, Xue Y, et al. Transition-metal-free synthesis of phenanthridinones from biaryl-2-oxamic acid under radical conditions. Organic Letters 2015;17:346-9.

19 Ingrassia L, Lefranc F, Dewelle J, Pottier L, Mathieu V, Spiegl-Kreinecker S, et al. Structure− activity relationship analysis of novel derivatives of narciclasine (an Amaryllidaceae isocarbostyril derivative) as potential anticancer agents. Journal of Medicinal Chemistry 2009;52:1100-14.

20 Van Goietsenoven G, Mathieu V, Lefranc F, Kornienko A, Evidente A, Kiss R. Narciclasine as well as other Amaryllidaceae Isocarbostyrils are Promising GTP-ase Targeting Agents against Brain Cancers. Medicinal research reviews 2013;33:439-55.

21 Fürst RJPm. Narciclasine–an amaryllidaceae alkaloid with potent antitumor and anti-inflammatory properties. Planta medica 2016;82:1389-94.

22 Hu Y, Zhang Z, Ye W, Zhang W, Hu M, Yuan W, et al. A DNA structure-mediated fluorescent biosensor for apurinic/apyrimidinic endonuclease 1 activity detection with ultra-high sensitivity and

749 selectivity. Sensors and Actuators B: Chemical 2021;330.
750 23 Pai MY, Lomenick B, Hwang H, Schiestl R, McBride W, Loo JA, et
751 al. Drug affinity responsive target stability (DARTS) for small-molecule
752 target identification. Methods Mol Biol 2015;1263:287-98.
753 24 Malinovska L, Cappelletti V, Kohler D, Piazza I, Tsai TH, Pepelnjak
754 M, et al. Proteome-wide structural changes measured with limited
755 proteolysis-mass spectrometry: an advanced protocol for high-throughput
756 applications. Nat Protoc 2023;18:659-82.
757 25 Wu X, Takenaka K, Sonoda E, Hochegger H, Kawanishi S,
758 Kawamoto T, et al. Critical roles for polymerase zeta in cellular tolerance
759 to nitric oxide-induced DNA damage. Cancer Res 2006;66:748-54.
760 26 Lamb J, Crawford ED, Peck D, Modell JW, Blat IC, Wrobel MJ, et al.
761 The Connectivity Map: using gene-expression signatures to connect small
762 molecules, genes, and disease. Science 2006;313:1929-35.
763 27 Cetin MH, Rieckmann T, Hoffer K, Riepen B, Christiansen S,
764 Gatzemeier F, et al. G2 checkpoint targeting via Wee1 inhibition
765 radiosensitizes EGFRvIII-positive glioblastoma cells. Radiat Oncol
766 2023;18:19.
767 28 Chen D, Hong R, Cao Y, Wu Q, Wang Y, Chen J, et al. Combined
768 Wee1 and EGFR inhibition reveals synergistic antitumor effect in
769 esophageal squamous cell carcinoma. Carcinogenesis 2023;44:451-62.
770 29 Gimple RC, Bhargava S, Dixit D, JN R. Glioblastoma stem cells:

lessons from the tumor hierarchy in a lethal cancer. Genes Dev 2019;33(11-12):591-609.

30 Suva ML, Tirosh I. The Glioma Stem Cell Model in the Era of Single-Cell Genomics. Cancer Cell 2020;37:630-6.

31 Liu Y, Zhou F, Ali H, Lathia JD, Chen P. Immunotherapy for glioblastoma: current state, challenges, and future perspectives. Cellular & Molecular Immunology 2024;21:1354-75.

32 Davis ME. Glioblastoma: Overview of Disease and Treatment. Clinical journal of oncology nursing 2016;20:S2-8.

33 Pearl LH, Schierz AC, Ward SE, Al-Lazikani B, Pearl FM. Therapeutic opportunities within the DNA damage response. Nature Reviews Cancer 2015;15:166-80.

34 Venugopal S, Sharma V, Mehra A, Singh I, Singh G. DNA intercalators as anticancer agents. Chem Biol Drug Des 2022;100:580-98.

35 Biebricher AS, Heller I, Roijmans RFH, Hoekstra TP, Peterman EJG, Wuite GJL. The impact of DNA intercalators on DNA and DNA-processing enzymes elucidated through force-dependent binding kinetics. Nature communications 2015;6:7304.

36 Martinez R, Chacón-García. L. The search of DNA-intercalators as antitumoral drugs: what it worked and what did not work. Current Medicinal Chemistry 2005;12:127-51.

37 Frattini V, Trifonov V, Chan JM, Castano A, Lia M, Abate F, et al. The

integrated landscape of driver genomic alterations in glioblastoma. Nature Genetics 2013;45:1141-9.

38 Li X-P, Guo Z-Q, Wang B-F, Zhao M. EGFR alterations in glioblastoma play a role in antitumor immunity reg ulation. Front Oncol;13.

39 Ghelli Luserna di Rorà A, Cerchione C, Martinelli G, Simonetti G. A WEE1 family business: regulation of mitosis, cancer progression, and therapeutic target. Journal of hematology & oncology 2020;13:126.

40 Lee A, Arasaratnam M, Chan DLH, Khasraw M, Howell VM, Wheeler H. Anti-epidermal growth factor receptor therapy for glioblastoma in adults. The Cochrane database of systematic reviews 2020;5:Cd013238.

41 Westphal M, Maire CL, Lamszus K. EGFR as a Target for Glioblastoma Treatment: An Unfulfilled Promise. CNS Drugs 2017;31:723-35.

42 Music D, Dahlrot RH, Hermansen SK, Hjelmborg J, de Stricker K, Hansen S, et al. Expression and prognostic value of the WEE1 kinase in gliomas. J Neurooncol 2016;127:381-9.

Figures

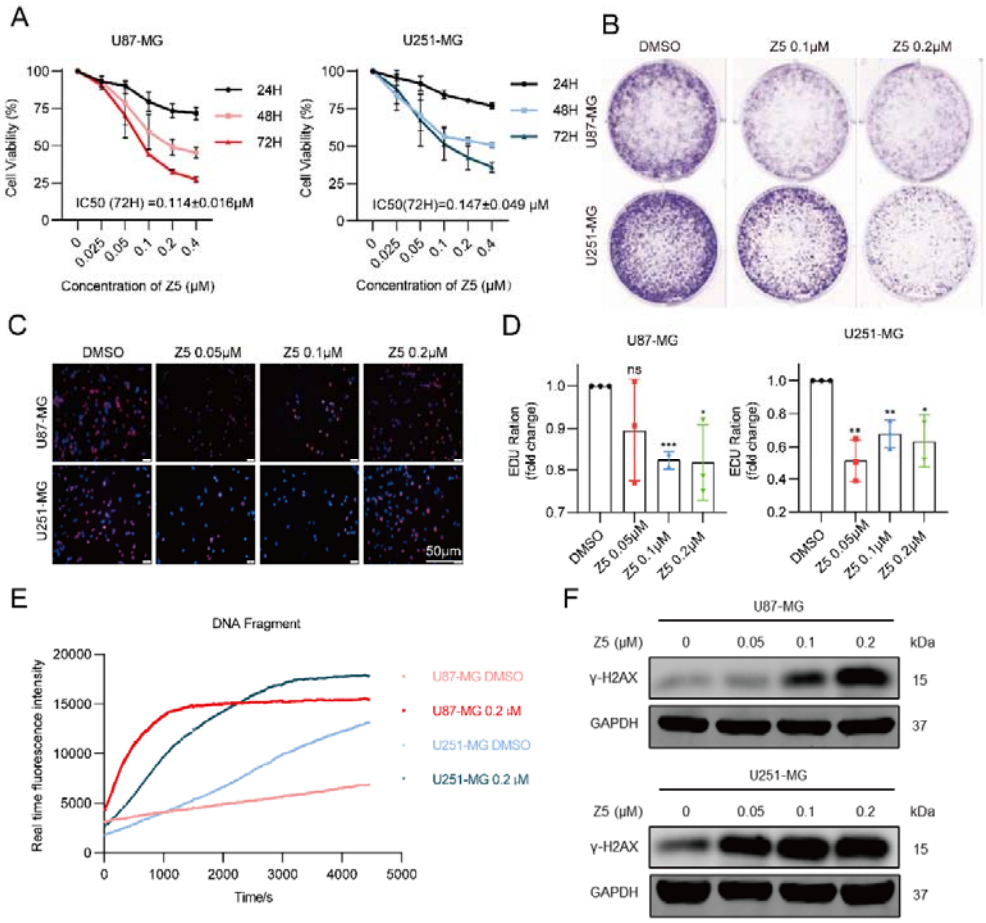

Figure 1 Z5 inhibits the proliferation and induces DNA damage in GBM cells. (A) Cell viability was evaluated using CCK-8 kit after treated with Z5 for 24h, 48h and 72h. (B) The efficacy of Z5 in a colony formation assay was evaluated. (C) Fluorescent images of proliferating GBM cell lines in various treatment conditions (red: EDU staining; blue: Hoechst staining). (D) Quantification of the fluorescence of each group. Data are presented as the mean ± SD, n=3, compared with DMSO group. (E) Effect of Z5 on DNA fragment. (F) The expression of γ-H2AX was

measured by immunoblotting after treatment with Z5.

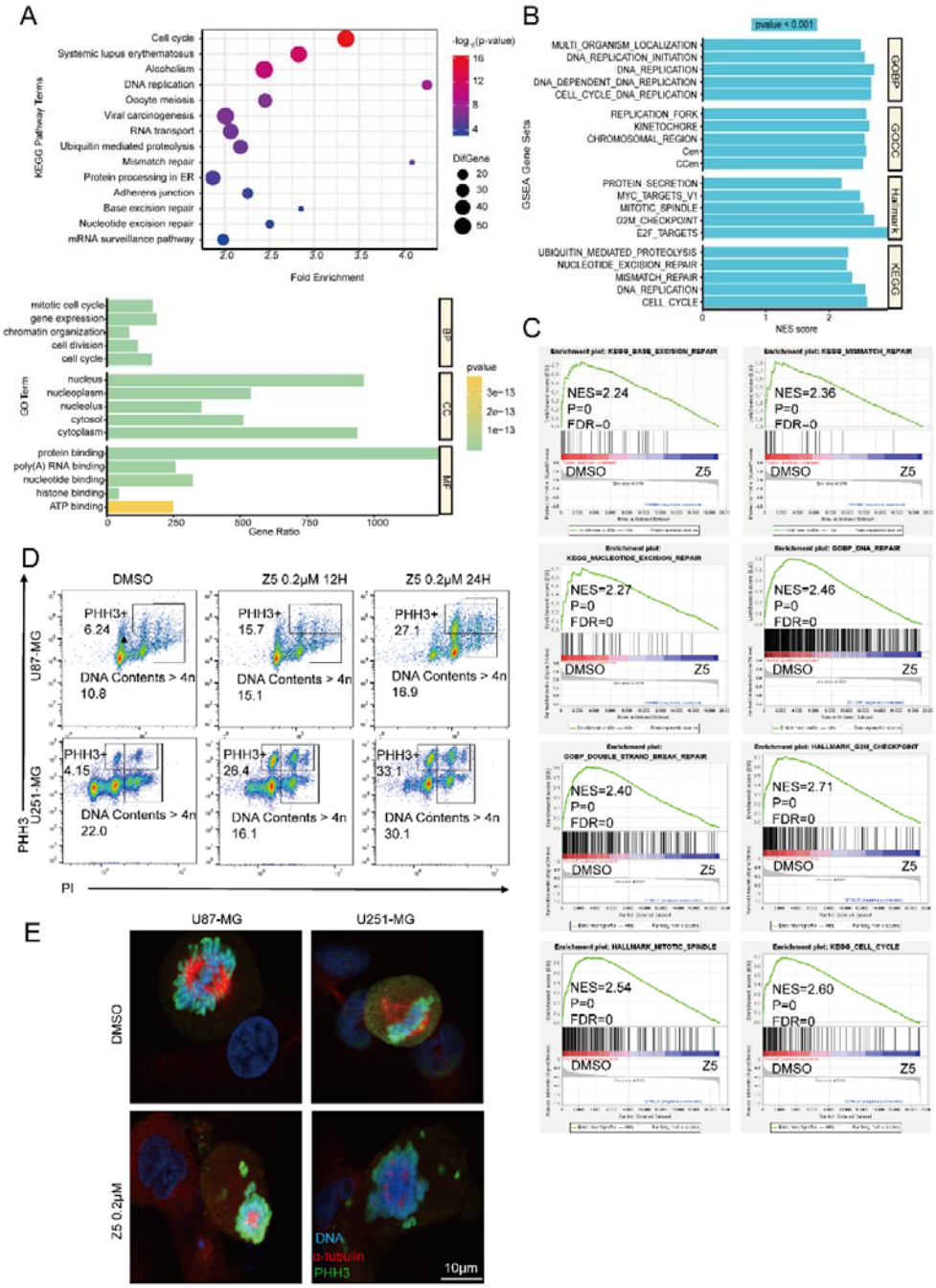

Figure 2 Z5 induces G2/M arrest and mitotic catastrophe in GBM cells. (A) KEGG pathway enrichment analysis and GO enrichment

analysis of downregulated genes identified by the U87-MG microarray. ER: Endoplasmic Reticulum. (B) GSEA analysis of all genes identified by the U87-MG microarray. Cen: chromosome centromeric region; CCen: condensed chromosome centromeric region. (C) GSEA analysis of base excision repair, mismatch repair, nucleotide excision repair, DNA repair, double strand break repair, G2M checkpoint, mitotic spindle and cell cycle pathways. (D) Representative flow cytometric analysis of PHH3+ and DNA contents > 4n cells. (E) Immunofluorescence staining was performed with anti-tubulin (Red), anti-PHH3 (Green) on the U87-MG and U251-MG cells treated with or without Z5.

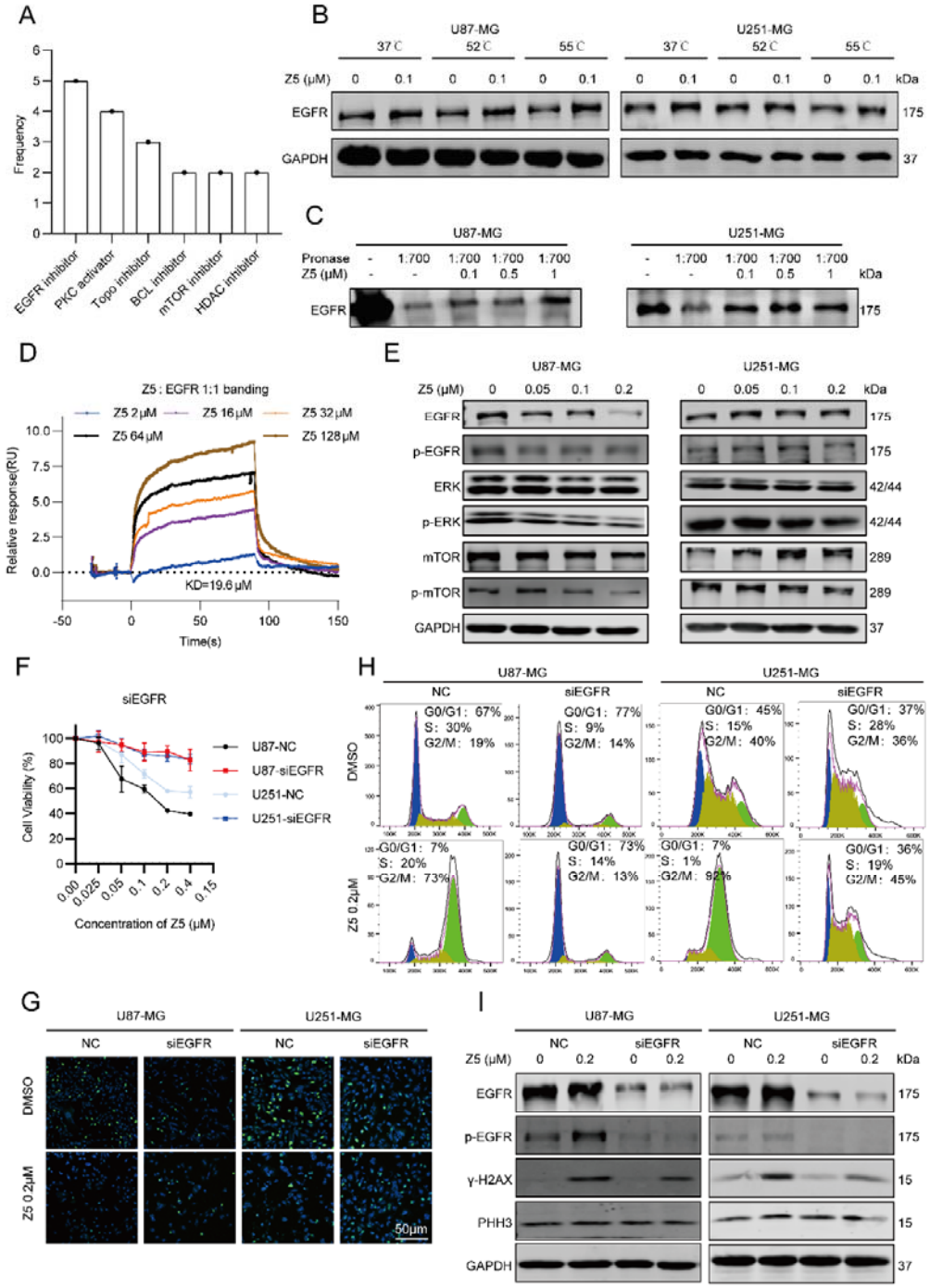

Figure 3 Z5 targets EGFR. (A) In the CMAP data, the top 10 compounds positively correlated with microarray data were selected for each cell type. The descriptions of these compounds were then

statistically analyzed, and the descriptions were ranked based on their frequency of occurrence. (B) The CETSA assay was used to evaluate the binding between Z5 (0.1mM) in thermodynamic levels. The expression of EGFR was detected by immunoblotting. (C) The DARTS assay was used to evaluate the binding between different concentrations of Z5. The expression of EGFR was detected by immunoblotting. (D) Interaction between Z5 and recombinant EGFR kinase domain protein was analyzed by SPR. (E) The expression of EGFR, p-EGFR, ERK, p-ERK, mTOR, p-mTOR in U87-MG and U251-MG cells were measured by immunoblotting after treatment with different concentrations of Z5 for 48h. (F) Growth curves of GBM cell lines transfected with or without si-EGFR and treated with or without Z5 for 48H. (G) The efficacy of Z5 on GBM cell lines transfected with or without si-EGFR was detected by EDU staining. (H) The cell cycle of GBM cell lines transfected with or without si-EGFR was evaluated using flow cytometry after being treated with or without Z5 for 24h. (I) The expression of EGFR, p-EGFR, γ-H2AX and PHH3 in U87-MG and U251-MG cells were measured by immunoblotting after treatmehhnt with Z5 for 48h.

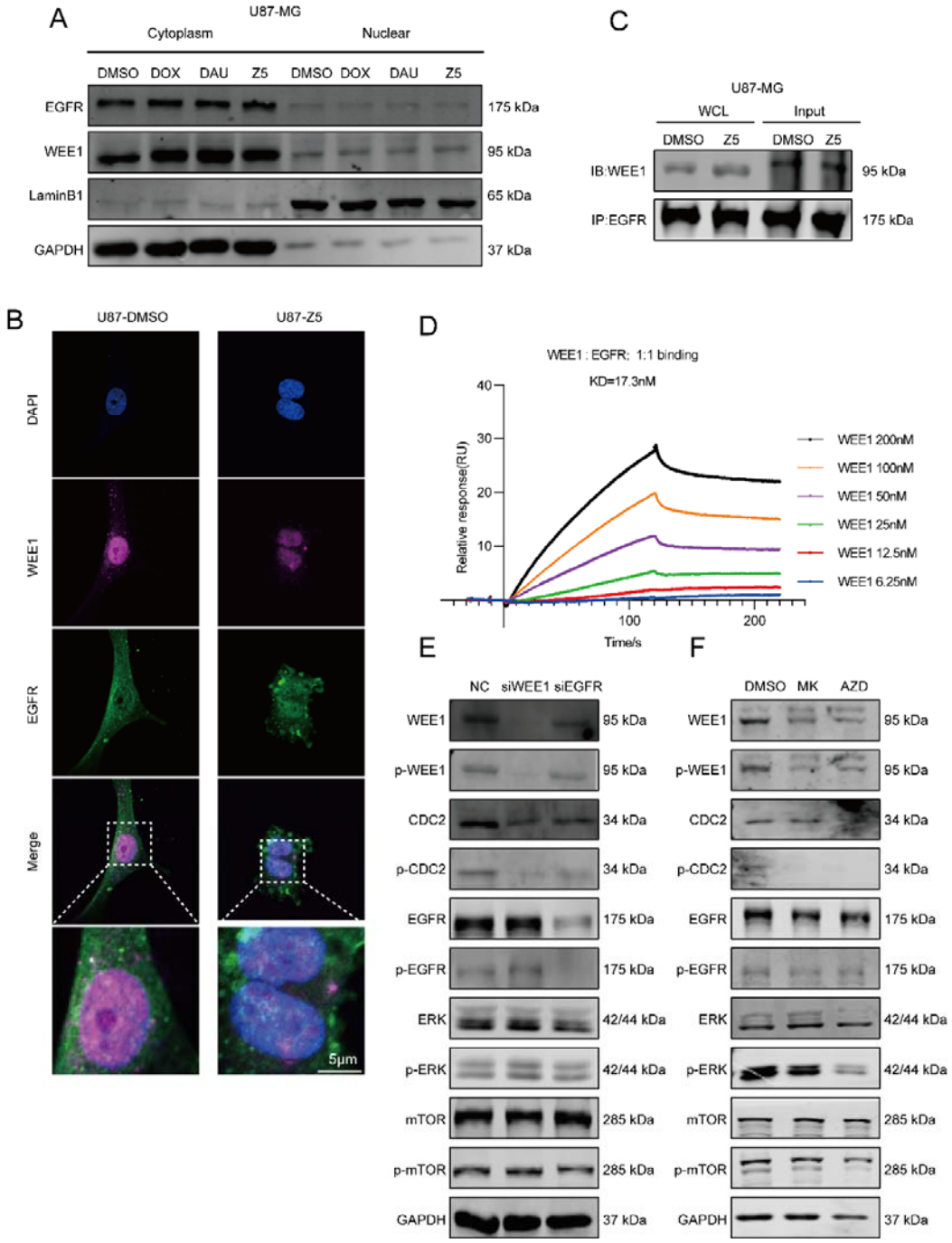

Figure 4 Z5 interferes with the interaction of EGFR with WEE1. (A) The expressions of EGFR and WEE1 in cytoplasm and nucleus were analyzed in U87-MG cells with or without of Z5 treatment after a 15-minute incubation. (B) Confocal immunofluorescence staining was

used to analyze the localization of EGFR and WEE1 after 15 minutes of Z5 treatment or untreated. (C) Co-immunoprecipitation was used to detect the interaction between EGFR and WEE1 after 15 min or untreated Z5 treatment. (D) Interaction between recombinant EGFR kinase domain proteins and recombinant WEE1 kinase domain proteins were analyzed by SPR. (E) The expressions level of WEE1, p-WEE1, CDC2, p-CDC2, EGFR, p-EGFR, ERK, p-ERK, mTOR, p-mTOR after U87-MG transfected with or without siRNA. (F) The expressions level of WEE1, p-WEE1, CDC2, p-CDC2, EGFR, p-EGFR, ERK, p-ERK, mTOR, p-mTOR after U87-MG treated with DMSO or MK1775 (4 μM) or AZD9291 (8 μM) for 48H.

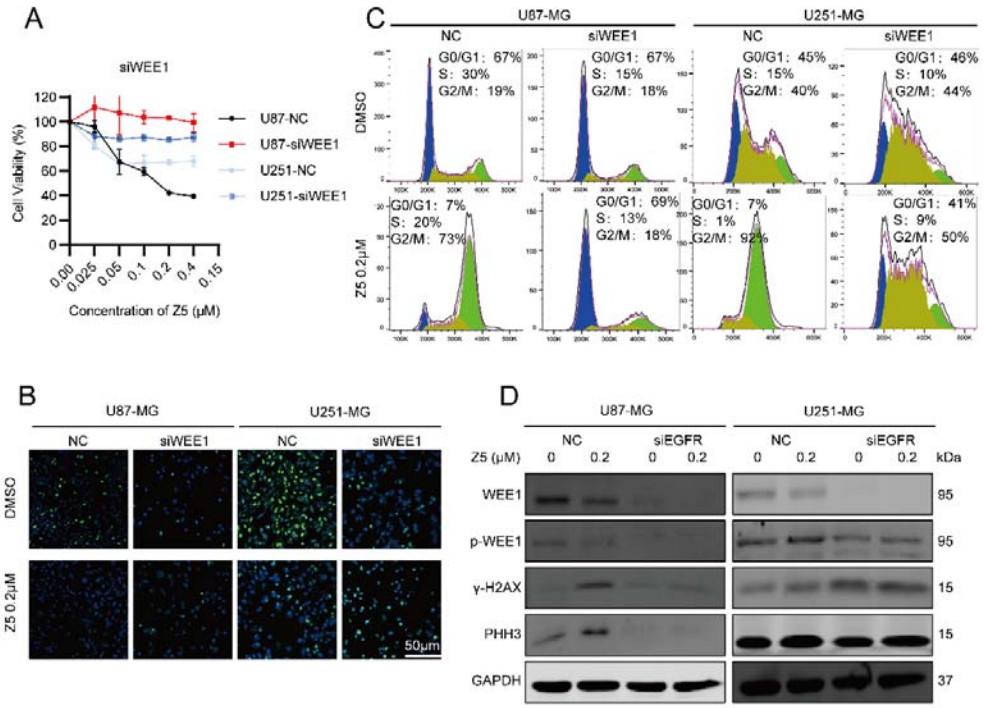

Figure 5 Silencing WEE1 significantly impairs the therapeutic efficacy of Z5. (A) Growth curves of GBM cell lines transfected with or without si-WEE1 and treated with or without Z5 for 48H. (B) The efficacy of Z5 on GBM cell lines transfected with or without si-WEE1 was detected by EDU staining. (C) The cell cycle of GBM cell lines transfected with or without si-WEE1 was evaluated using flow cytometry after being treated with Z5 for 24h. (D) The expression of WEE1, p-WEE1, γ-H2AX and PHH3 in U87-MG and U251-MG cells were measured by immunoblotting after treatment with Z5 for 48h.

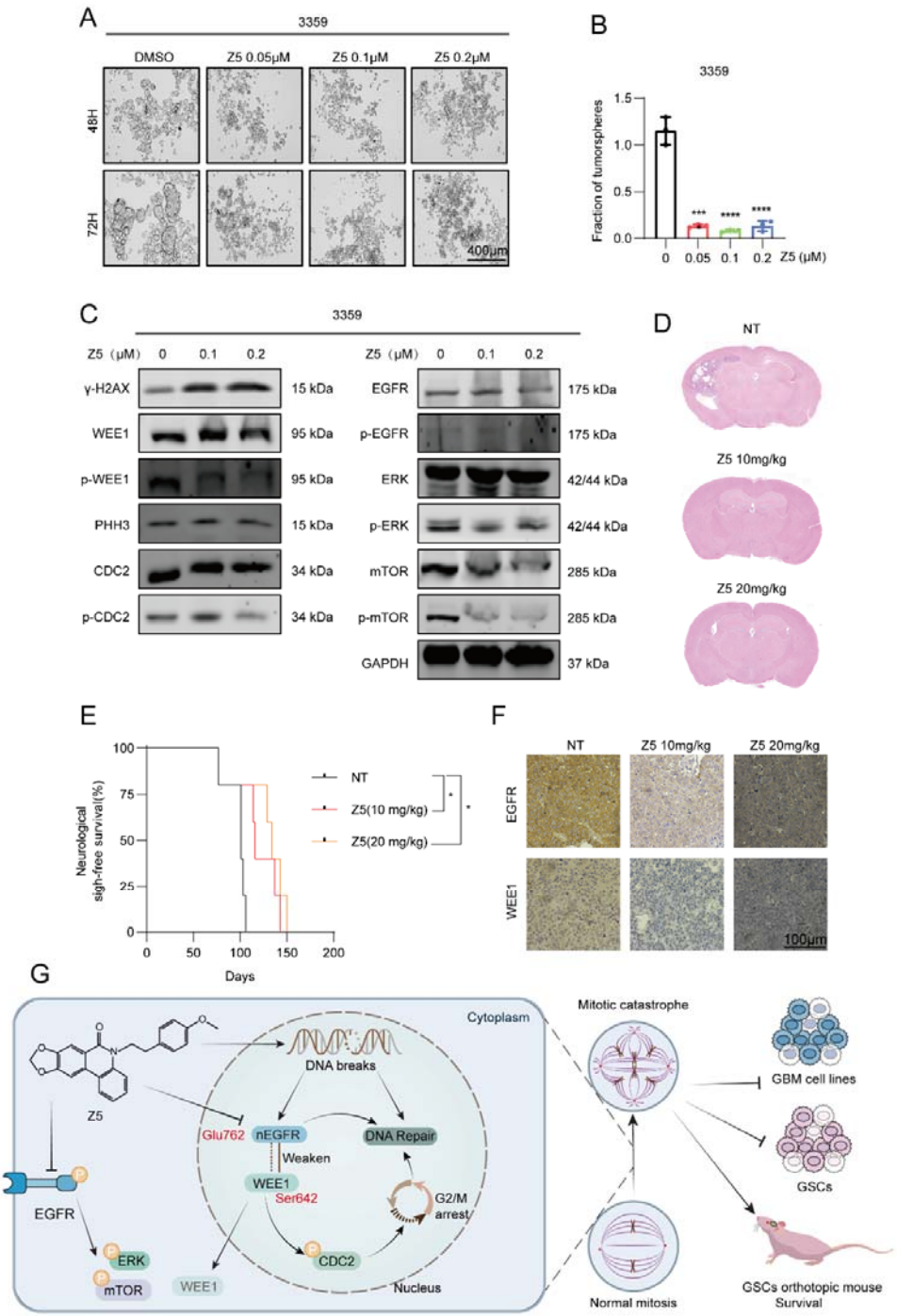

Figure 6 Z5 suppresses the proliferation of patient-derived GSCs in vitro and in vivo. (A) Microscopic observation of GSC-derived tumor sphere formation in 3359 cells after incubation with different

concentrations of Z5 for 48 hours. (B) Quantitative analysis of the fragmentation of tumor spheres from (A). Data are presented as the mean ± SD, n=3, ****$p < 0.0001$, compared with “0” group. (C) The expressions level of γ-H2AX, WEE1, p-WEE1, PHH3, CDC2, p-CDC2, EGFR, p-EGFR, ERK, p-ERK, mTOR, p-mTOR in 3359 treated with or without Z5. (D) H&E staining to evaluate intracranial tumor formation. (E) Survival analysis of mice with orthotopically transplanted GSCs. Data are presented as the mean ± SD, n=4, *$p < 0.05$, compared with NT group. (F) Immunohistochemistry examination of EGFR and WEE1 expression in orthotopic xenografts in mice. (G) Detailed molecular mechanisms of Z5-mediated anti-GBM effects through targeting EGFR and WEE1.